Hydrostatic Adjustment: Lamb's Problem

PETER R. BANNON

Department of Meteorology, The Pennsylvania State University, University Park, Pennsylvania

(Manuscript received 18 July 1994, in final form 21 November 1994)

ABSTRACT

The prototype problem of hydrostatic adjustment for large-scale atmospheric motions is presented. When a horizontally infinite layer of compressible fluid, initially at rest, is instantaneously heated, the fluid is no longer in hydrostatic balance since its temperature and pressure in the layer have increased while its density remains unchanged. The subsequent adjustment of the fluid is described in detail for an isothermal base-state atmosphere.

The initial imbalance generates acoustic wave fronts with trailing wakes of dispersive acoustic gravity waves. There are two characteristic timescales of the adjustment. The first is the transit time it takes an acoustic front to travel from the source region to a particular location. The second timescale, the acoustic cutoff frequency, is associated with the trailing wake. The characteristic depth scale of the adjustment is the density scale height. If the depth of the heating is small compared with the scale height, the final pressure perturbation tends to zero and the pressure field adjusts to the initial density field. For larger depths, there is a mutual adjustment of the pressure and density fields.

Use of the one-dimensional analogue of the conservation of Ertel's potential vorticity removes hydrostatic degeneracy and determines the final equilibrium state directly. As a result of the adjustment process, the heated layer has expanded vertically. Since the region below the layer is unaltered, the region aloft is displaced upward uniformly. As a consequence of the expansion, the pressure and temperature anomalies in the layer are reduced from their initial values immediately after the heating. Aloft both the pressure and density fields are increased but there is no change in temperature. Since the base-state atmosphere is isothermal, warm advection is absent; since the vertical displacements of air parcels is uniform aloft, compressional warming is also absent.

The energetics of the adjustment are documented. Initially all the perturbation energy resides in the heated layer with a fraction $\gamma^{-1} = 71.4\%$ stored as available potential energy, while the remainder is available elastic energy. A fraction $\kappa = R/C_p = (\gamma - 1)/\gamma = 28.6\%$ of the initial energy is lost to propagating acoustic modes. Here $\gamma = C_p/C_v$ is the ratio of the specific heats and R is the ideal gas constant. The remainder of the energy is partitioned between the heated layer and the region aloft. The energy aloft appears mostly as elastic energy, and the energy in the layer appears mostly as available potential energy.

1. Introduction

Large-scale atmospheric motions display an approximate hydrostatic balance in which vertical accelerations are small, and there is a force balance on an individual air parcel between the upward pressure gradient force and the downward acceleration due to gravity. Traditional scale analyses (e.g., Phillips 1990) indicate that the hydrostatic approximation is valid for low-frequency, shallow disturbances for which the frequency is much less than the buoyancy frequency and the aspect ratio of the flow is small. These conditions, however, do not address the mechanisms whereby a fluid adjusts to a state of hydrostatic balance.

The purpose of this paper is to discuss the prototype problem of hydrostatic adjustment. The problem was originally advanced by Lamb (1908) [see also Lamb (1932), sections 309 and 310] who considered a single point source of hydrostatic imbalance. Here we show that a heating of finite vertical extent will generate a dipole of imbalance. The vertical asymmetries introduced by the dipole are examined. We also extend Lamb's treatment to include a consideration of the structure of the final equilibrium state and of the energetics of the system.

Several factors motivate this study. Foremost of these is the fact that the mutual adjustment of the density, temperature, and pressure fields toward hydrostaticity is a fundamental process of large-scale atmospheric motions and is thus of intrinsic physical interest. In contrast, convective systems display and maintain large nonhydrostatic features. The study of hydrostatic adjustment seeks to understand both the mechanisms for the achievement of balance as well as those for failure. Such investigations are particularly appropriate in light of recent advances in computer technology that make feasible nonhydrostatic numerical weather prediction (e.g., Dudhia 1993; Warner et al. 1992).

Corresponding author address: Dr. Peter R. Bannon, Department of Meteorology, The Pennsylvania State University, 503 Walker Building, University Park, PA 16802-5013.

Section 2 describes the model physics and the linearized equations of motion. The generation of the initial state of imbalance by an instantaneous heating is presented. Section 3 presents the results for the transient solution, building upon the analysis of Lamb (1908). Section 4 shows that the final state can be obtained directly using the conservation of the one-dimensional analogue to potential vorticity. This one-dimensional adiabatic invariant is derived in the appendix for the nonlinear case. This invariant, the specific stability, removes the problem of hydrostatic degeneracy. Section 5 summarizes a calculation of the energetics. Section 6 concludes the paper with a qualitative discussion of the general three-dimensional adjustment problem.

2. The model

The model atmosphere is a stably stratified, inviscid, diatomic, ideal gas in a Cartesian coordinate system where $-g\mathbf{k}$ is the acceleration due to gravity. The isothermal resting base state is denoted with the subscript nought. The linearized equations of motion for one-dimensional, small-amplitude perturbations are

$$\rho_0 \frac{\partial w'}{\partial t} = -\frac{\partial p'}{\partial z} - \rho' g, \tag{2.1}$$

$$\frac{\partial \rho'}{\partial t} + w' \frac{d\rho_0}{dz} + \rho_0 \frac{\partial w'}{\partial z} = 0, \tag{2.2}$$

$$\frac{\partial \theta'}{\partial t} + w' \frac{d\theta_0}{dz} = \dot{\Theta}, \tag{2.3}$$

$$\frac{\theta'}{\theta_0} = \frac{p'}{\gamma p_0} - \frac{\rho'}{\rho_0}, \tag{2.4}$$

$$\frac{p'}{p_0} = \frac{\rho'}{\rho_0} + \frac{T'}{T_0}, \tag{2.5}$$

where a prime denotes a perturbation quantity. The notation is standard; $\gamma = C_p/C_v = 7/5$ is the ratio of the specific heats at constant pressure and volume. The isothermal base state satisfies

$$\rho_0 = \rho_* e^{-z/H_s}, \quad p_0 = p_* e^{-z/H_s},$$
$$T_0 = T_*, \quad \theta_0 = T_* e^{+\kappa z/H_s}, \tag{2.6}$$

where the asterisk subscript denotes a constant reference value. The scale height is

$$H_s = \frac{RT_0}{g}, \tag{2.7}$$

with R the ideal gas constant and $\kappa = R/C_p$. Note that the set (2.1)–(2.5) is unaffected by the inclusion of rotation about the $\mathbf{k}$ axis.

The potential temperature warming $\dot{\Theta}$ represents the effect of the diabatic processes. For weak heating

$$\dot{\Theta} = \frac{\theta_0}{\rho_0 C_p T_0} Q, \tag{2.8}$$

where Q is the heating rate per unit volume. The heating is taken to be uniform in the layer $-a < z < +a$ and to occur instantaneously at the time $t = 0$. Mathematically, Q is described by

$$Q = \frac{C_v}{R} \Delta p [H(z + a) - H(z - a)] \delta(t), \tag{2.9}$$

where δ is the Dirac delta function and H is the Heaviside step function. For definiteness the constant Δp is assumed positive; then (2.9) describes a warming. Note that the origin of the coordinate system, $z = 0$, lies at the center of the region of heating and does not correspond to a bounding lower surface. Then by (2.6) the reference values (denoted by the asterisk subscript) correspond to those of the base-state variables at the center of the region of heating.

The perturbation fields are taken to be zero just before the heating (e.g., $t = 0^-$). Immediately after the heating (e.g., $t = 0^+$) the fields are

$$p'(t = 0^+) = \Delta p [H(z + a) - H(z - a)], \tag{2.10}$$

$$T'(t = 0^+) = \Delta T e^{+z/H_s} [H(z + a) - H(z - a)], \tag{2.11}$$

$$\theta'(t = 0^+) = (\Delta T/\gamma) e^{+(1+\kappa)z/H_s} \times [H(z + a) - H(z - a)], \tag{2.12}$$

$$\rho'(t = 0^+) = 0, \quad \text{and} \quad w'(t = 0^+) = 0, \tag{2.13}$$

where $\Delta T = T_0(\Delta p/p_*)$. The initial response is confined to the layer $-a < z < +a$ where the heating has created a uniform pressure perturbation of amplitude Δp. The temperature is warmed differentially due to the decrease in the base-state density with height. The perturbation density, however, remains unchanged and no motion has yet developed.

These initial conditions represent a state of hydrostatic imbalance. We seek a solution of the subsequent evolution of the atmosphere and a description of the final equilibrium.

3. Transient solution

The subsequent evolution of the fluid is described by the adiabatic form of (2.1)–(2.5). The vertical motion field satisfies

$$\frac{\partial^2 w'}{\partial t^2} = -\frac{c^2}{H_s} \frac{\partial w'}{\partial z} + c^2 \frac{\partial^2 w'}{\partial z^2}, \tag{3.1}$$

or, with $w'(z, t) = e^{+z/2H_s} w(z, t)$,

$$\frac{\partial^2 w}{\partial t^2} = -N_A^2 w + c^2 \frac{\partial^2 w}{\partial z^2}, \tag{3.2}$$

where

$$N_A = \frac{c}{2H_s} \quad \text{and} \quad c = (\gamma R T_0)^{1/2} \tag{3.3}$$

are the acoustic cutoff frequency and the speed of sound, respectively. The initial conditions for w' are

$$w'(t = 0^+) = 0, \tag{3.4a}$$

$$\rho_0 \left.\frac{\partial w'}{\partial t}\right|_{t=0^+} = -\left.\frac{\partial p'}{\partial z}\right|_{t=0^+}$$

$$= -\Delta p[\delta(z + a) - \delta(z - a)]. \tag{3.4b}$$

The latter condition results from the substitution of (2.10) and (2.13) into the momentum equation (2.1). Vertical motions are excited at the top and bottom of the heated layer where the hydrostatic imbalance is concentrated. Henceforth we refer to the levels $z = \pm a$ as the source regions.

Solutions of (3.2) subject to (3.4) are well known (e.g., Lamb 1908; Cahn 1945; Gill 1982). One finds

$$w'(z, t) = \Delta w e^{+z/2H_s}[e^{+a/2H_s}W(z - a, t) - e^{-a/2H_s}W(z + a, t)], \tag{3.5}$$

where $\Delta w = \Delta p/(2\rho_* c)$ and

$$W(z, t) = H(c^2t^2 - z^2)J_0\left[N_A\left(t^2 - \frac{z^2}{c^2}\right)^{1/2}\right]. \tag{3.6}$$

Here J_0 is the zero-order Bessel function. Plots of (3.6) appear in Gill (1982, Figs. 7.3b and 7.4) with the substitutions $f \leftrightarrow N_A$ and $a \leftrightarrow 2H_s$.

Most of the physics of the transients contained in (3.5) can be ascertained by analogy with section 7.3 of Gill. Each source region generates a pair of wave fronts of instantaneous vertical acceleration followed by oscillatory wakes. The disturbances propagate both upward and downward from each source. The disturbances from the upper source initially generate rising motion as the front passes; the lower source generates sinking motion. This dipole behavior reflects the reversal of the vertical pressure gradient force from the upper to the lower source.

Several features of the solution are unique to the hydrostatic adjustment problem. The solution (3.5) displays the well-known exponential increase with height associated with the conservation of wave energy. More importantly, the upper source generates a stronger perturbation in the vertical motion field than the lower source. Despite the fact that the pressure gradients at the two sources have the same amplitude, the upper fluid, by virtue of its smaller ambient density, undergoes greater initial accelerations than the denser fluid at the lower source. The net difference in the density and hence in the acceleration is given by the factor $\exp(2a/H_s)$, which agrees with the relative weighting of the terms in (3.5). This asymmetry is crucial to the hydrostatic adjustment problem and is the ultimate explanation for the asymmetry displayed in the final equilibrium.

The nature of the asymmetry is seen in Fig. 1. Immediately after $t = 0^+$, the fluid at the upper source $z = +a$ is accelerated upward to velocity $\Delta w e^{+a/Hs}\mathbf{k}$ by the wave front of the upper source. The wave front from the lower source arrives at $t = 2a/c$ and decelerates the fluid to velocity $\Delta w(e^{-a/Hs} - 1)\mathbf{k}$. Conversely, the fluid at the lower source $z = -a$ is first accelerated downward with velocity $-\Delta w e^{-a/Hs}\mathbf{k}$ and then upward to $\Delta w(1 - e^{-a/Hs})\mathbf{k}$ at $t = 2a/c$ as the wave front from the upper source arrives. The fluid in the middle of the heating lies quiescent until $t = a/c$ when the wave fronts from the upper and lower sources arrive simultaneously to accelerate the fluid to $\Delta w(e^{+a/Hs} - e^{-a/Hs})\mathbf{k}$. The subsequent oscillatory motion arises from the sum of the trailing wakes. As time progresses the frequency of the oscillation approaches N_A and the fluid oscillates more in phase.

4. Final equilibrium

The final equilibrium state should satisfy the steady-state form of (2.1)–(2.3):

$$0 = -\frac{\partial p'}{\partial z} - \rho' g, \tag{4.1}$$

$$w'\frac{d\rho_0}{dz} + \rho_0\frac{\partial w'}{\partial z} = 0, \tag{4.2}$$

$$w'\frac{d\theta_0}{dz} = 0, \tag{4.3}$$

as well as (2.4) and (2.5). The first equation states that the final state is in hydrostatic balance. The third equa-

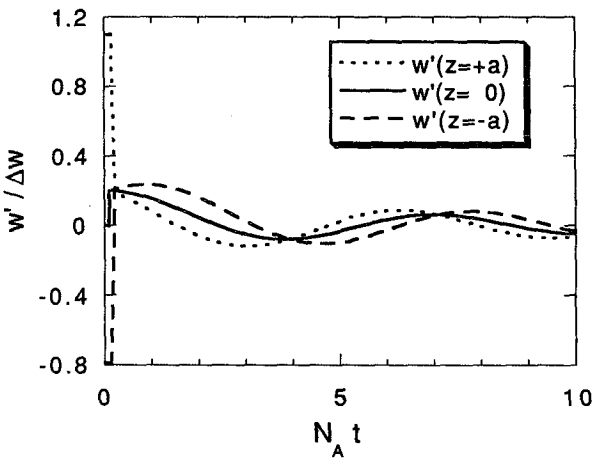

FIG. 1. A schematic of the temporal variation of the perturbation vertical motion field as a function of time at the top ($z = +a$) and bottom ($z = -a$) source regions and in the middle ($z = 0$) of the heated layer.

tion implies that the perturbation vertical motion vanishes, $w' = 0$. Then the second equation is trivially satisfied, and the mathematical problem for the final distribution of the mass and pressure fields becomes ill posed. This situation is one of hydrostatic degeneracy and is analogous to geostrophic degeneracy (Pedlosky 1987, 55–56): there is insufficient information to distinguish the correct solution out of the infinity of possible solutions, all of which exhibit hydrostatic balance.

The degeneracy is removed by the following invariant of the motion. The vertical motion field can be eliminated from the continuity equation (2.2) and the adiabatic heat equation (2.3) to yield

$$\frac{\partial}{\partial t}\left[\frac{\partial}{\partial z}\left(\frac{\rho_0\theta'}{d\theta_0/dz}\right) - \rho'\right] = 0. \tag{4.4}$$

This conservation statement can also be derived from the linearized form of the general nonlinear result (see appendix) that the specific stability σ,

$$\sigma \equiv \frac{1}{\rho}\frac{\partial\theta}{\partial z}, \tag{4.5}$$

is conserved for adiabatic flow. We note that σ is the one-dimensional analogue of Ertel's potential vorticity. The result (4.4) also follows if one starts from the general, linearized, three-dimensional adjustment problem and then takes the limit as the horizontal variations vanish.

Integrating (4.4) from $t = 0^+$ to $t = \infty$ yields

$$+\frac{\partial}{\partial z}\left(\frac{\rho_0\theta_f'}{d\theta_0/dz}\right) - \rho_f' = +\frac{\partial}{\partial z}\left(\frac{\rho_0\theta_i'}{d\theta_0/dz}\right), \tag{4.6}$$

where the subscripts i and f refer to the initial and final states, respectively. Here θ_i' is given by (2.12) and the final state variables satisfy (4.1), (2.4), and (2.5). Expressing (4.6) in terms of the final pressure perturbation yields

$$\frac{d^2p_f'}{dz^2} + \frac{1}{H_s}\frac{dp_f'}{dz} = \frac{\Delta p}{\gamma H_s}[\delta(z+a) - \delta(z-a)], \tag{4.7}$$

or, letting $p_f' \equiv e^{-z/2H_s}p(z)$,

$$\frac{d^2p}{dz^2} - \frac{p}{4H_s^2} = e^{+z/2H_s}\frac{\Delta p}{\gamma H_s}[\delta(z+a) - \delta(z-a)].$$

This equation is readily solved using standard techniques. The solution for p_f' that is bounded at $z = \pm\infty$ is

$$p_f' = \frac{\Delta p}{\gamma}\begin{cases} 2\sinh\left(\dfrac{a}{H_s}\right)e^{-z/H_s}, & z \geq +a, \\ 1 - e^{-(z+a)/H_s}, & -a \leq z \leq +a, \\ 0, & z \leq -a. \end{cases} \tag{4.8}$$

It can also be shown that (4.8) holds if there is a flat rigid boundary below the heated layer at, say, $z = -b < -a$. At such a boundary, $w' = 0$, and the heat equation (2.3) implies that θ' is conserved so $\theta_f' = \theta_i'$ at $z = -b$. Since no mass leaves the fluid column in this one-dimensional problem, $p_f'(z = -b) = 0$. Use of these conditions again leads to (4.8).

The solutions are for the other variables in the final state are

$$\mathrm{gr}_f' = \frac{\Delta\rho}{\gamma}\begin{cases} \mathrm{h}\left(\dfrac{a}{H_s}\right)e^{-z/H_s}, & z \geq +a, \\ -e^{-(z+a)/H_s}, & -a \leq z \leq +a, \\ 0, & z \leq -a, \end{cases} \tag{4.9}$$

$$T_f' = \frac{\Delta T}{\gamma}e^{+z/H_s}\begin{cases} 0, & z \geq +a, \\ 1, & -a \leq z \leq +a, \\ 0, & z \leq -a, \end{cases} \tag{4.10}$$

$$\theta_f' = \frac{\Delta T}{\gamma}e^{+(1+\kappa)z/H_s} \times \begin{cases} -2\kappa\sinh\left(\dfrac{a}{H_s}\right)e^{-z/H_s}, & z \geq +a, \\ 1 - \kappa(1 - e^{-(z+a)/H_s}), & -a \leq z \leq +a, \\ 0, & z \leq -a, \end{cases} \tag{4.11}$$

where $\Delta\rho = \Delta p/gH_s$. Inspection of (4.8)–(4.11) indicates that the characteristic depth scale of the solution is the scale height H_s.

Figure 2 depicts the attributes of the final state in relation to the initial conditions. Unlike the initial field, the final pressure perturbation varies continuously with height and no infinite pressure gradients exist. The pressure perturbation is positive both in and above the heated layer with a maximum at the top of the layer. Its amplitude in the layer is less than its initial value. The maximum of $(\Delta p/\gamma)(1 - e^{-2a/Hs})$ lies at the top of the heated layer. For small a/H_s, the final pressure perturbation tends to zero and the pressure field has adjusted to the initial density field ($\rho_i' = 0$). For large a/H_s there is a mutual adjustment.

The redistribution of mass (Fig. 2b) during the adjustment process leads to a decrease in density in the layer of heating with an increase aloft. This distribution is consistent hydrostatically with the increase in pressure with height in the layer and with the decrease with height aloft. Note that the vertical integral of the density anomaly vanishes and thus mass is conserved.

The final temperature perturbation (Fig. 2c) shows an identical structure as the initial field but is reduced by a factor of $\gamma^{-1} \sim 71\%$. The potential temperature perturbation (Fig. 2d) also shows a decrease in the layer of heating. Unlike the T' field, however, the θ' field shows a nonzero response aloft with a negative perturbation that increases with height.

The features of the final state reflect the conservation of potential vorticity (4.4). The top hat heating profile

generates two delta-function anomalies in the potential vorticity field. The negative upper anomaly (at $z = +a$) is stronger than the positive anomaly below (at $z = -a$). The vertical asymmetry is a consequence of the increase of potential temperature with height. In both the initial and the final states this potential vorticity distribution manifests itself in the discontinuity in the θ' field at the source regions.

One salient feature of the final state is that the fluid below the layer of heating is unaltered from its initial state. The downward-propagating acoustic modes have no lasting influence on the fluid below the layer of heating and propagate away to $z = -\infty$ (or else are absorbed or reflected by a lower bounding surface). Only the fluid in and above the layer is affected by the adjustment process. This asymmetry stems directly from the asymmetry displayed by the transient solution (3.5).

Insight into the role of the transient acoustic modes in generating the final state can be gleaned by calculation of the net vertical displacement ζ_f' of a fluid parcel. Since the initial parcel displacement is zero, the final displacement is the integrated effect of the vertical motion field:

$$\zeta_f'(z) = \int_0^\infty w'(z, t)dt. \tag{4.12}$$

The integral I for each source region has the form

$$I(z) \equiv \int_0^\infty W(z, t)dt$$

$$= \int_{|z|/c}^\infty J_0\left[N_A\left(t^2 - \frac{z^2}{c^2}\right)^{1/2}\right]dt, \tag{4.13}$$

or, defining $x \equiv N_A(t^2 - z^2/c^2)^{1/2}$,

$$I(z) = \frac{1}{N_A}\int_0^\infty \frac{xJ_0(x)}{\left(x^2 + \frac{z^2}{4H_s^2}\right)^{1/2}}dx$$

$$= \frac{1}{N_A}e^{-|z|/2H_s}, \tag{4.14}$$

where the latter integral has been evaluated using the results in Gradshteyn and Ryzhik (1980, p. 682). The net effect of the wave disturbance falls off exponentially with distance from the source region. This behavior reflects the thinning of the initial wave pulse due to dispersion (see Gill's Fig. 7.4) The result is

$$\zeta_f' = \Delta\zeta e^{+z/2H_s}[e^{+a/2H_s}e^{-|z-a|/2H_s} - e^{-a/2H_s}e^{-|z+a|/2H_s}], \tag{4.15}$$

or

$$\zeta_f' = \Delta\zeta\begin{cases} 2\sinh\left(\frac{a}{H_s}\right), & z \geq +a, \\ e^{+z/H_s} - e^{-a/H_s}, & -a \leq z \leq +a, \\ 0, & z \leq -a, \end{cases} \tag{4.16}$$

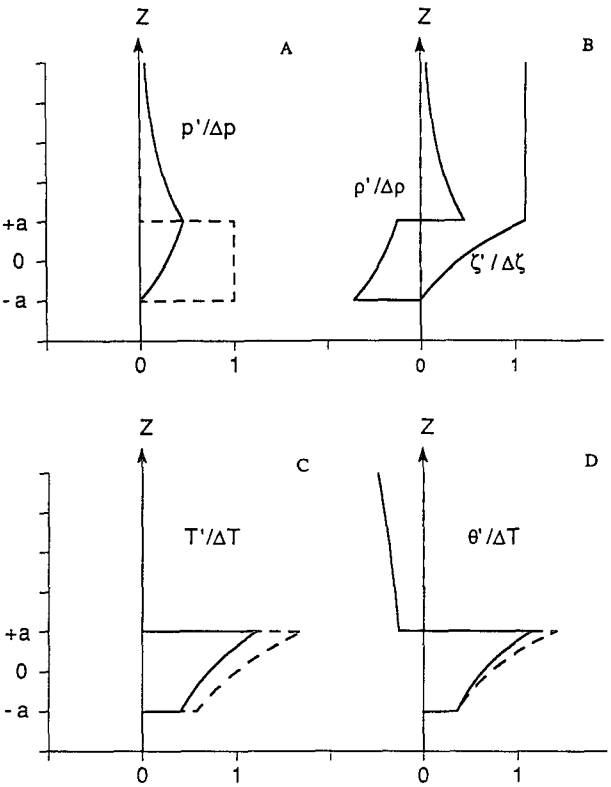

FIG. 2. A schematic diagram of the perturbation fields as a function of height. The solid curves refer to the final state; dashed curves refer to the initial state immediately after the heating.

where $\Delta\zeta = \Delta w/N_A = \Delta p/(\gamma\rho_* g)$. The amplitude of the displacement is proportional to the product of the strength of the disturbance in the vertical motion field Δw and the acoustic time N_A^{-1}.

The vertical displacement can also be derived using two alternative approaches. One is the adiabatic method where the heat equation in the form

$$\frac{\partial\theta'}{\partial t} = -\frac{\partial\zeta}{\partial t}\frac{d\theta_0}{dz}$$

is integrated from $t = 0^+$ to $t = \infty$ to obtain

$$\zeta_f' = +\frac{g}{N_0^2}\frac{\theta_i' - \theta_f'}{\theta_0}.$$

This result is identical to (4.16) but requires knowledge of the initial and final potential temperature perturbations, (2.12) and (4.11), respectively. The second method follows Richardson (1922), who derived a diagnostic equation for the vertical motion field w_R assuming hydrostatic balance. The linearized form of his equation suitable for the present problem is

$$\frac{\partial w_R}{\partial z} = \frac{R}{C_p}\frac{Q}{p_s}.$$

Integration with respect to time from $t = 0^-$ to $t > 0$ and vertically upward from $z < -a$ yields (4.16). This method finds the displacement directly from the heating but provides no information on the timescale of the adjustment. Lastly, we note that, since the heating is horizontally uniform, the diagnostic omega equation predicts no vertical motion or displacement.

The result (4.16) is depicted in Fig. 2b. At and below the base of the heated layer, the net vertical displacement vanishes and $\zeta_f' = 0$. This result holds for either heating or cooling. The wave disturbance from the upper source is just strong enough to negate the tendency of the disturbance from the lower source to produce a net downward displacement. This perfect compensation stems from the interplay of two competing processes; the upper source generates a stronger w' field since the fluid is lighter aloft, but its effect on the displacement decays with distance according to (4.14). Above the lower source the disturbance from the upper source dominates and the ζ_f' increases monotonically with height from $z = -a$. The maximum displacement occurs right at and above the upper source at $z = +a$. This structure indicates that the heated layer has expanded, leading to a uniform displacement of the fluid aloft.

The features of the final state can be explained in light of the structure of the vertical displacement field. Integration with respect to time of the continuity equation in the form

$$\frac{\partial \rho'}{\partial t} = -\frac{\partial(\rho_0 w')}{\partial z} \tag{4.17}$$

yields

$$\rho_f' = -\frac{\partial(\rho_0 \zeta_f')}{\partial z} = -\zeta_f' \frac{\partial \rho_0}{\partial z} - \rho_0 \frac{\partial \zeta_f'}{\partial z}. \tag{4.18}$$

Then the density below the layer of heating is unchanged. In the layer, the fluid expansion $\partial\zeta_f'/\partial z$ dominates the advection of heavy fluid from below, and the density perturbation is reduced. Above the layer the vertical displacement is constant with height and the density perturbation increases as a result of the advection of heavier fluid from below. This advection decreases with height as the density decays exponentially with height. With this density perturbation the pressure perturbation follows by integration of the hydrostatic equation. The final thermal fields may be written in the form

$$T_f' = T_i' - T_0(\gamma - 1)\frac{\partial \zeta_f'}{\partial z}, \tag{4.19}$$

$$\theta_f' = \theta_i' - \zeta_f' \frac{\partial \theta_0}{\partial z}. \tag{4.20}$$

The decrease in the temperature perturbation from its initial diabatically generated anomaly arises from the work done by the ambient pressure field during the expansion of the air in the layer $-a < z < +a$. Because the base state is isothermal, there is no warm advection associated with vertical displacements. Alternatively, the decrease in the potential temperature perturbation from its initial value arises from adiabatic cooling due to ascent.

5. Energetics

Energy conservation for the perturbation is given by the equation

$$\frac{\partial}{\partial t}\left[\frac{\rho_0 w'^2}{2} + \frac{\rho_0}{2N_0^2}\left(\frac{g\theta'}{\theta_0}\right)^2 + \frac{p'^2}{2\rho_0 c^2}\right] = -\frac{\partial(p'w')}{\partial z}, \tag{5.1}$$

which states that the local time rate of change of the total energy per unit volume is given by the rate of work done by the pressure perturbation in accelerating and compressing an air parcel. The total energy is the sum of the three terms in the square bracket. The first is the kinetic energy per unit volume. There is no standard terminology for the second and third terms. Here we refer to them as the available potential energy and the available elastic energy. [Eckart (1960) labels them the thermobaric and elastic energies, respectively, while Gill (1982) collectively calls them the available potential energy.]

The available potential and elastic energies per unit area are

$$\text{APE} \equiv \int \frac{\rho_0}{2N_0^2}\left(\frac{g\theta'}{\theta_0}\right)^2 dz = E_0 \int e^{\hat{z}} \hat{\theta}^2 d\hat{z}, \tag{5.2}$$

$$\text{AEE} \equiv \int \frac{p'^2}{2\rho_0 c^2} dz = (\gamma - 1)E_0 \int e^{\hat{z}} \hat{p}^2 d\hat{z}, \tag{5.3}$$

where $\hat{z} = z/H_s$, $E_0 = (\Delta p)^2/(2\gamma^2 \rho_* N_0^2 H_s)$, $\hat{p} = p'/\Delta p$, and

$$\hat{\theta} = (\theta'/\Delta\theta) \quad \text{where} \quad \Delta\theta = \theta_0(\Delta p/\gamma p_0). \tag{5.4}$$

We focus on the energy difference between the initial ($t = 0^+$) and the final ($t = \infty$) states. The kinetic energy is identically zero for both states. Initially all the energy resides in the layer $-a < z < +a$ as available and elastic. One finds

$$\text{APE}_i = 2E_0 \sinh(\hat{a}), \tag{5.5}$$

$$\text{AEE}_i = 2(\gamma - 1)E_0 \sinh(\hat{a}), \tag{5.6}$$

and the total energy is

$$\text{TE}_i \equiv \text{APE}_i + \text{AEE}_i = 2\gamma E_0 \sinh(\hat{a}), \tag{5.7}$$

where $\hat{a} = a/H_s$. A fraction, $\gamma^{-1} = 71.4\%$, is stored as available potential energy; the remainder, $\kappa = (\gamma - 1)/\gamma = 28.6\%$, is stored as available elastic energy. The energy stored increases exponentially with the depth of the heated layer.

The initial energy distribution (5.5) and (5.6) is consistent with the generation G of energy by the heating. This generation is

$$G = \int_{t=0}^{t=0^+} \int \left[\rho_0 \frac{g\theta'}{\theta_0} \left(\frac{g\hat{\Theta}/\theta_0}{N_0^2} \right) + p' \frac{\hat{\Theta}}{\theta_0} \right] dz dt$$
$$= 2E_0 \sinh\hat{a} + 2(\gamma - 1)E_0 \sinh\hat{a}$$
$$= 2\gamma E_0 \sinh\hat{a}, \quad (5.8)$$

where the principal value for the perturbation [i.e., half of (2.10) and (2.12)] is used in evaluating the time integral. The heating generates both potential and elastic energies as given by the first two terms in (5.8).

In the final state, energy resides both in and above the heated layer. Above the layer one finds

$$\mathrm{APE}_f = 4\left(\frac{\gamma - 1}{\gamma}\right)^2 E_0 \sinh^2(\hat{a}) e^{-\hat{a}}, \quad (5.9a)$$

$$\mathrm{AEE}_f = 4\left(\frac{\gamma - 1}{\gamma^2}\right) E_0 \sinh^2(\hat{a}) e^{-\hat{a}}, \quad (5.9b)$$

$$\mathrm{TE}_f = 4\left(\frac{\gamma - 1}{\gamma}\right) E_0 \sinh^2(\hat{a}) e^{-\hat{a}}, \quad (5.9c)$$

and in the layer

$$\mathrm{APE}_f = 2\gamma^{-2} E_0 \{ [1 + (\gamma - 1)^2 e^{-2\hat{a}}] \sinh(\hat{a}) + 2\hat{a}(\gamma - 1)e^{-\hat{a}} \}, \quad (5.10a)$$

$$\mathrm{AEE}_f = 2(\gamma - 1)\gamma^{-2} E_0 [\sinh(2\hat{a}) - 2\hat{a}] e^{-\hat{a}}, \quad (5.10b)$$

$$\mathrm{TE}_f = 2\gamma^{-2} E_0 \{ [1 + (\gamma - 1)^2 e^{-2\hat{a}}] \sinh(\hat{a}) + (\gamma - 1)e^{-\hat{a}} \sinh(2\hat{a}) \}. \quad (5.10c)$$

The total energy in the final state is the sum of (5.9c) and (5.10c), or

$$\mathrm{TE}_f = 2E_0 \sinh(\hat{a}). \quad (5.11)$$

The energy propagated away in the form of acoustic waves is given by the difference between (5.7) and (5.11), or

$$E_{\mathrm{waves}} = 2(\gamma - 1)E_0 \sinh(\hat{a}). \quad (5.12)$$

Thus, a constant fraction, $\kappa = (\gamma - 1)/\gamma = 28.6\%$, of the initial energy is lost to propagating acoustic modes. A fraction,

$$\frac{\gamma - 1}{\gamma^2}(1 - e^{-2\hat{a}}) \leqslant \frac{\gamma - 1}{\gamma^2} = 20.4\%, \quad (5.13)$$

of the initial energy eventually resides above the layer originally heated. This fraction increases with the depth of the layer. The remainder, a fraction

$$\frac{[1 + (\gamma - 1)e^{-2\hat{a}}]}{\gamma^2} \leqslant \frac{1}{\gamma} = 71.4\%, \quad (5.14)$$

of the total lies in the layer.

The partitioning of the energy is summarized in Fig. 3 where the energies (5.9), (5.10), and (5.12) are normalized by the total initial energy (5.7) and plotted as a function of $\hat{a} = a/H_s$. Since energy is conserved, their normalized total is unity. The crosses on the right ordinate denote the asymptotic values as $\hat{a} \to \infty$. For example, the normalized elastic energy in the heated layer is given by (5.10b) divided by (5.7) or

$$\left(\frac{\gamma - 1}{\gamma^3}\right) \frac{[\sinh(2\hat{a}) - 2\hat{a}]}{\sinh(\hat{a})} e^{-\hat{a}} \sim \left(\frac{\gamma - 1}{\gamma^3}\right)$$
$$= 0.146 \quad \text{as} \quad \hat{a} \to \infty. \quad (5.15)$$

In the heated layer most of the energy is in the form of potential energy, but this fraction decreases with the layer thickness a. In contrast most of the energy aloft, a fixed fraction $\gamma^{-1} = 5/7$, resides in the form of elastic energy.

6. Conclusions

We have reexamined the classical problem of Lamb (1908) for the vertical propagation of acoustic waves using the concepts of adjustment theory. It has been shown that differential heating in the vertical produces a hydrostatic imbalance. Acoustic modes are excited that mutually redistribute the mass and pressure fields to obtain a final state of hydrostatic balance. The salient features of the adjustment are summarized in the abstract. The summary as well as the discussion in the

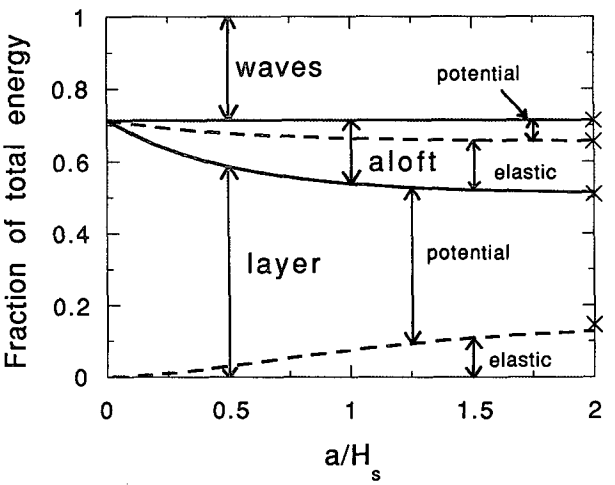

FIG. 3. Energy partitioning as a function of the heating half-width a. The solid curves separate the final energy contained in the heated layer and aloft as well as that lost to acoustic waves. The dashed curves indicate the fraction of available elastic energy. The crosses along the right-hand ordinate indicate the asymptotic values of the curves.

text assumes the heating is positive. Since the problem is linear, the solution for cooling is found by a reversal in sign. For example, a cooled layer contracts during the adjustment process, the region aloft is displaced downward, and the region below the cooling is again unaltered.

The present idealized study isolates some of the essential physics of the problem. The use of the top hat heating profile is mathematically convenient but produces a discontinuity of pressure. [Gill's (1982) adjustment problem has a similar shortcoming.] This unrealistic feature can be eliminated by convolution using a heating profile with a smoothly varying profile. The results of the final equilibrium state are also valid for general heating profiles since the solution of (4.7) represents the Green's function for the problem.

The base-state atmosphere has been assumed to be isothermal. Lamb (1908; 1932, section 310) briefly discusses the case of a basic state with a linear temperature gradient. The transient behavior of the acoustic modes is qualitatively similar for short timescales before the waves are reflected off the finite top of the atmosphere. A qualitative difference with the isothermal case would be the generation of a nonzero temperature perturbation aloft due to thermal advection.

The major assumption has been the restriction to the one-dimensional case of horizontal homogeneity. The absence of a vertical displacement in the final state of the lower layer is a direct consequence of the horizontal homogeneity. Applications for this geometry would include the relatively uniform radiative cooling of the troposphere in clear-sky situations and the latent heating in a deck of stratus clouds.

Inferences drawn from the present study are now made about the general three-dimensional problem. Following Monin and Obukhov (1959) we consider the small-amplitude motions in an isothermal, uniformly rotating fluid whose dispersion relation is

$$\omega\left[\left(\frac{f^2-\omega^2}{c^2}+k^2+l^2\right)(N^2-\mu\omega^2) + (f^2-\omega^2)(m^2+\Gamma^2)\right]=0, \quad (6.1)$$

for a plane wave pressure perturbation of the form

$$p' \sim e^{[i(kx+ly+mz-\omega t)]}e^{-(z/2H_s)}, \quad (6.2)$$

where $\Gamma = 3/14H_s$, and $N^2 = \kappa g/H_s$ is the square of the buoyancy frequency. Here μ is a flag introduced by Monin and Obukhov to denote the presence ($\mu = 0$) or absence ($\mu = 1$) of the hydrostatic approximation. The dispersion relation (6.1) contains acoustic modes ($\omega > N_A = 1.11N$) and inertia–gravity waves ($\omega < N$), a Lamb wave ($m^2 = -\Gamma^2$), and the stationary hydrostatic–geostrophic mode ($\omega = 0$).

In general, an arbitrary diabatic warming will generate an initial condition that is in neither hydrostatic nor geostrophic balance. Monin and Obukhov (p. 161) note that "the initial field can be represented as the sum of the stationary and wave components. As time passes, the wave disturbances disappear and at any finite area of the field it approaches the stationary type corresponding to" geostrophic and hydrostatic balance. Since setting the flag $\mu = 0$ filters out the acoustic modes and describes hydrostatic balance, they conclude that the acoustic modes are responsible for the hydrostatic adjustment and that the timescale is "several minutes" based on the time it takes an acoustic mode to pass through the depth of the atmosphere. This interpretation needs some refinement, however.

The adjustment process can be subdivided into stages according to the various classes of waves. For example there will be an acoustic adjustment that involves the radiating away of the acoustic modes from the initial source. The present study describes the prototype calculation of the *acoustic* hydrostatic adjustment. It complements Cahn's (1945) calculation of the Rossby problem for the geostrophic adjustment by hydrostatic gravity waves.

To explore the effects of three dimensionality, consider the Gedanken experiment in which a portion of the atmosphere with vertical and horizontal scales D and L, respectively, is suddenly made warmer than its environment. Traditional scale analyses (Pedlosky 1987; Phillips 1990) indicate that the atmospheric response will depend upon the value of the aspect ratio $\delta = D/L$ for the blob of fluid in question. A "plume" (i.e., a tall buoyant prolate blob with $\delta \gg 1$) will respond nonhydrostatically; a "pancake" (i.e., an oblate blob with $\delta \ll 1$) will respond hydrostatically.

The differences in the two responses for $\delta \ll 1$ and $\delta \gg 1$ can be interpreted from the dispersion relation (6.1) with $f = 0$. Figure 4 shows the isopleths of frequency ω as a function of the horizontal wavenumber $K_H = (k^2 + l^2)^{1/2}$ and vertical wavenumber m for a range of scales on the synoptic and mesoscale. The group velocity $\mathbf{c}_g = \nabla_k\omega$ is indicated schematically by the arrows. The diagram is symmetric about both the abscissa and ordinate. For the pancake $\delta = D/L \sim K_H/m \ll 1$ and the modes close to the ordinate will be preferentially excited. This region of wavenumber space corresponds to typical scales of large-scale meteorology and large-scale numerical weather prediction. Inspection of the diagram indicates that only the acoustic modes have significant vertical energy propagation; the gravity waves propagate horizontally. Thus, there will be a rapid acoustic adjustment in the vertical followed by a slower gravity adjustment in the horizontal. Since the gravity waves near the ordinate have $\omega^2 \ll N^2$ they are essentially hydrostatic. Thus, the acoustic adjustment yields a hydrostatically balanced state, which then adjusts toward geostrophic balance.

The adjustment is different for a plume with $\delta \gg 1$. In this case the modes close to the abscissa in Fig. 4

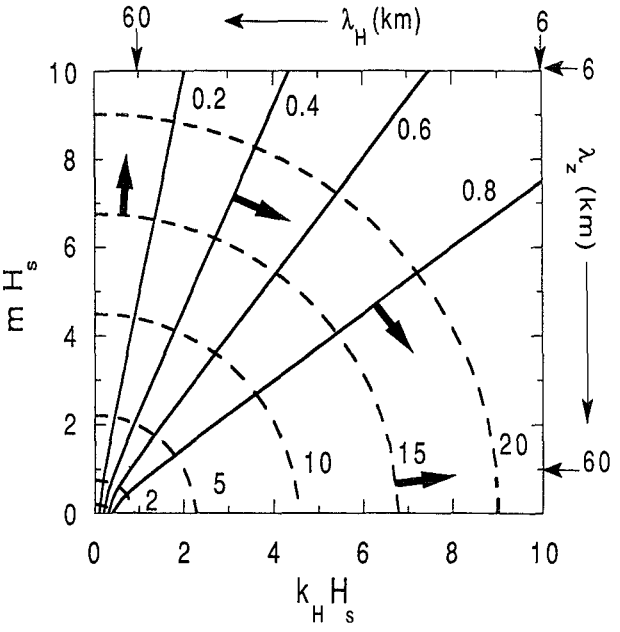

FIG. 4. Schematic contour plot of the scaled frequency ω/N as a function of the scaled horizontal $K_H H_s$ and vertical mH_s wavenumbers for the acoustic (dashed) and gravity modes (solid) for the nonrotating form of (6.1). Here N is the buoyancy frequency and H_s is the scale height for an isothermal atmosphere. Typical wavelengths are indicated along the right and top sides of the plot. For large wavenumbers the gravity curves become straight lines; the acoustic curves become circles. A plot for small wavenumbers appears in Gill (1982). The arrows indicate the direction of the group velocity, which is directed normal to the curves toward higher frequency.

will be excited. Then the acoustic adjustment will occur rapidly in the horizontal followed by a nonhydrostatic wave adjustment in the vertical. The one-dimensional horizontal acoustic adjustment in the absence of gravity has been described by, for example, Lighthill (1978). More recently Nicholls and Pielke (1994) have discussed it with regard to thunderstorm dynamics. Thus, the relative roles of the acoustic and gravity modes have been interchanged from those for the pancake with $\delta \ll 1$.

The intermediate case of $\delta \sim 1$ will have features of both extreme cases. There will be a rapid acoustic hydrostatic adjustment with timescale N_A^{-1} followed by a nonacoustic hydrostatic adjustment with timescale N^{-1} associated with nonhydrostatic gravity waves. Lastly, a slow geostrophic adjustment with timescale f^{-1} will be accomplished by the hydrostatic gravity waves. We note that the relative contribution of these modes depends on the details of the forcing function and how it projects onto the various modes. Dickinson (1969a,b) discusses the Green's function solution for this general case.

The results of the present study are pertinent to the design and testing of nonhydrostatic numerical models. In addition to finite-differencing approximations in space and time, numerical models include additional simplifications (e.g., a rigid upper boundary, computational retardation of the vertical acoustic modes, a time-splitting scheme that treats the acoustic modes separately). One common assumption (Klemp and Wilhelmson 1978; Dudhia 1993) is the neglect of the heating term in the pressure equation. This neglect leads to heating at constant pressure rather than constant volume. The reduction in heating is $\kappa = R/C_p = 28\%$, an amount consistent with that lost to acoustic waves for horizontally homogeneous heating. Dudhia (1993) notes that this neglect can compensate for the presence of a rigid upper boundary that prohibits the free expansion described here by the displacement (4.16).

It is important to determine whether a numerical model simulates the physics of the adjustment adequately and, say, does not overadjust toward hydrostatic balance. A strong tendency to overadjust would probably negate a model's ability to capture the nonhydrostatic behavior of a particular weather phenomena. Thus, tests should be performed to determine the model configuration (e.g., in terms of time step, grid design, horizontal and vertical grid spacing and their ratio) that best emulates the analytic results.

The present analysis is also relevant to the choice of a set of "soundproof" equations. Such anelastic equations should display an instantaneous acoustic hydrostatic adjustment that is consistent with (4.8)–(4.11) with an apparent energy loss of 28%. This issue is discussed in Bannon (1995).

Acknowledgments. The author thanks J. Michael Fritsch for his encouragement. The author benefited from discussions with Jimy Dudhia, Dean Duffy, and George W. Platzman.

APPENDIX

An Invariant of One-Dimensional Adiabatic Flow

The nonlinear continuity and heat equations may be written in the form

$$\frac{D \ln(\rho)}{Dt} = -\frac{\partial w}{\partial z}, \tag{A1}$$

$$\frac{D\theta}{Dt} = \dot{\Theta}, \tag{A2}$$

where

$$\frac{D}{Dt} \equiv \frac{\partial}{\partial t} + w\frac{\partial}{\partial z} \tag{A3}$$

is the one-dimensional material derivative. Taking the derivative of (A2) with respect to z yields

$$\frac{D}{Dt}\left[\ln\left(\frac{\partial\theta}{\partial z}\right)\right] + \frac{\partial w}{\partial z} = \frac{\partial\dot{\Theta}/\partial z}{\partial\theta/\partial z}. \tag{A4}$$

By using (A1) to eliminate the vertical divergence one obtains

$$\rho \frac{D}{Dt}\left(\frac{1}{\rho}\frac{\partial \theta}{\partial z}\right) = \frac{\partial \dot{\Theta}}{\partial z}. \tag{A5}$$

Thus, the specific stability,

$$\sigma \equiv \frac{1}{\rho}\frac{\partial \theta}{\partial z}, \tag{A6}$$

is conserved for one-dimensional adiabatic motion.

REFERENCES

Bannon, P. R., 1995: Potential vorticity conservation, hydrostatic adjustment, and the anelastic approximation. *J. Atmos. Sci.*, **52,** (12) in press.

Cahn, A., 1945: An ihvestigation of the free oscillations of a simple current system. *J. Meteor.*, **2,** 113–119.

Dickinson, R. E., 1969a: Propagators of atmospheric motions. 1. Excitation by point impulses. *Rev. Geophys. Space Phys.*, **7,** 483–514.

——, 1969b: Propagators of atmospheric motions. 2. Excitation by switch-on sources. *Rev. Geophys. Space Phys.*, **7,** 515–538.

Dudhia, J., 1993: A nonhydrostatic version of the Penn State–NCAR mesoscale model: Validation tests and simulation of an Atlantic cyclone and cold front. *Mon. Wea. Rev.*, **121,** 1493–1513.

Eckart, C., 1960: *Hydrodynamics of Oceans and Atmospheres.* Pergamon Press, 290 pp.

Gill, A. E., 1982: *Atmosphere–Ocean Dynamics.* Academic Press, 662 pp.

Gradshteyn, I. S., and I. M. Ryzhik, 1980: *Table of Integrals, Series, and Products.* Academic Press, 1160 pp.

Klemp, J. B., and R. B. Wilhelmson, 1978: The simulation of three-dimensional convective storm dynamics. *J. Atmos. Sci.*, **35,** 1070–1096.

Lamb, H., 1908: On the theory of waves propagated vertically in the atmosphere. *Proc. London Math. Soc.*, **7,** 122–141.

——, 1932: *Hydrodynamics.* Dover, 738 pp.

Lighthill, M. J., 1978: *Waves in Fluids.* Cambridge University Press, 504 pp.

Monin, A. S., and A. M. Obukhov, 1959: A note on the general classification of motions in a baroclinic atmosphere. *Tellus,* **11,** 159–162.

Nicholls, M. E., and R. A. Pielke, 1994: Thermal compression waves. *Quart. J. Roy. Meteor. Soc.*, **120,** 305–359.

Pedlosky, J., 1987: *Geophysical Fluid Dynamics.* Springer-Verlag, 710 pp.

Phillips, N. A., 1990: *Dispersion Processes in Large-Scale Weather Prediction.* World Meteorological Organization, 126 pp.

Richardson, L. F., 1922: *Weather Prediction by Numerical Process.* Cambridge University Press, 236 pp.

Warner, T. T., Y. H. Kuo, J. D. Doyle, J. Dudhia, D. R. Stauffer, and N. L. Seaman, 1992: Nonhydrostatic, mesobeta-scale, real-data simulations with the Penn State University/National Center for Atmospheric Research Mesoscale Model. *Meteor. Atmos. Phys.*, **49,** 209–227.